International Journal of Nanomedicine

Dovepress
Taylor & Francis Group

Open Access Full Text Article

ORIGINAL RESEARCH

Green Synthesis and Characterization of Silver Nanoparticles Using *Anchusa Officinalis*: Antimicrobial and Cytotoxic Potential

Cumali Keskin[1], Seyhan Aslan[2], Mehmet Fırat Baran[3], Ayşe Baran[4], Aziz Eftekhari[5,6], Mehmet Tevfik Adıcan[7], Elham Ahmadian[8], Sevki Arslan[9], Ali Jimale Mohamed[10]

[1]Department of Medical Services and Techniques, Vocational School of Health Services, Mardin Artuklu University, Mardin, Turkiye; [2]Department of Biology, Graduate Education Institute, Mardin Artuklu University, Mardin, 47200, Turkiye; [3]Department of Food Technology, Vocational School of Technical Sciences, Batman University, Batman, Turkiye; [4]Department of Plant and Animal Production, Medicinal and Aromatic Plants Program, Kiziltepe Vocational School, Marin Artuklu University, Mardin, Turkiye; [5]Department of Biochemistry, Faculty of Science, Ege University, Izmir, Turkiye; [6]Engineered Biomaterials Research Center, Department of Life Sciences, Khazar University, Baku, Azerbaijan; [7]Department of Electricity and Energy, Vocational School, Mardin Artuklu University, Mardin, Turkiye; [8]Kidney Research Center, Tabriz University of Medical Sciences, Tabriz, Iran; [9]Department of Biology, Faculty of Science, Pamukkale University, Denizli, Turkiye; [10]Department of Pharmacology, Faculty of Medicine, Somali National University, Mogadishu, 801, Somalia

Correspondence: Cumali Keskin, Department of Medical Services and Techniques, Vocational School of Health Services, Mardin Artuklu University, Mardin, 47100, Turkiye, Tel +905327413989, Email ckeskinoo@gmail.com; Ali Jimale Mohamed, Department of Pharmacology, Faculty of Medicine, Somali National University, Mogadishu, 801, Somalia, Email alijimamohamed@gmail.com

Objective: *Anchusa officinalis* L. (*A. officinalis*) is a herbaceous traditional medicinal plant used in the treatment of some diseases. The presence of its medicinal properties suggested that *A. officinalis* (AO) leaf extract could be used as a coating agent for the environmentally friendly production of silver nanoparticles (AgNPs).

Methods: The synthesized biogenic silver nanoparticles (AO-AgNPs) were characterized using different techniques. The antimicrobial activity of AgNPs against common bacterial pathogenic strains was determined by the minimum inhibitory concentration (MIC) method. The presence of phytochemicals was determined by LSMS/MS. The MTT assay was used to investigate AO-AgNPs' cytotoxic activity in malignant (LnCap, Caco2, MDA-MB2, A549) and healthy (HEK-293) cell lines.

Results: LC-MS/MS analysis detected the presence of rich phytochemicals that may be responsible for reduction reactions. Biogenic AO-AgNPs exhibited effective inhibition of the growth of pathogenic microorganisms at low concentrations. The most effective antimicrobial activity was measured as 0.5 µg/mL MIC against *S. aureus, E. coli*, and *C. albicans*. Moreover, AO-AgNPs showed significant inhibition on the growth of cancerous cell lines, especially at a concentration of 25 µg/mL. On the contrary, it was determined that the inhibition rate decreased in the growth of healthy cell lines due to the increase in concentration. The lowest EC_{50} values were determined as 15.15 µg/mL in A549 cells.

Conclusion: The obtained results showed that AO could be an important source for the synthesis of AgNPs. Especially their ability to inhibit the growth of antibiotic-resistant pathogenic bacteria at low concentrations compared to common antibiotics indicates that AO-AgNPs can be used as biomedical agents in various areas. Moreover, their suppressive effect on cancerous cell lines showed that they have the potential to be used as an anticancer agent, but due to their proliferative effect on healthy cell lines, care should be taken in determining the appropriate dose.

Keywords: *Anchusa officinalis*, antimicrobial activity, cytotoxic activity, biochemical composition, green synthesis, Ag NPs

Introduction

The biological synthesis of metallic nanoparticles uses bacteria, fungi, yeast, and plants to produce nanoscale particles. The "green synthesis" concept replaces dangerous chemicals and harmful byproducts with an eco-friendly and sustainable alternative. Biological substances or their extracts reduce and stabilize metal ions in a precursor solution to synthesize metallic nanoparticles. This produces nanoparticles with exact dimensions and shapes.[1–5]

Received: 9 December 2024
Accepted: 3 April 2025
Published: 12 April 2025

Nanotoxicology has grown, using conventional, standardized methodologies to measure NPs toxicity. However, standardization in assessment methods like test models (cell line, microbial species, and animal species) and exposure conditions (dosage intervals, AgNPs concentration range, duration of exposure, cell density, and animal weight) is needed to correlate research groups. However, minimum toxicity is unclear. The lack of a reference NPs system for evaluation may explain this. Despite multiple research groups reporting AgNP-based cytotoxicity and genotoxicity, in vitro test results can differ from in vivo test results, making them therapeutically irrelevant. AgNPs used in biomedical applications are not yet standardized; therefore, public exposure levels are unknown.[6]

The main reason for miniaturizing nanotechnology materials is research on their composition and properties. Synthesized metallic nanoparticles (MNPs) have properties that depend on their size and shape. Nanotechnology has advanced greatly in recent years, incorporating it into much of human life. Nanoparticles have mechanical, electrical, magnetic, physical, and chemical properties due to their large surface areas and small diameters. Metallic nanoparticles have these traits.[6–10]

Researchers have found numerous nanoscale metallic material synthesis methods. Green-way (biosynthesis) nanoparticle synthesis is a promising alternative to physical and chemical methods due to its simplicity, lack of toxicity, affordability, environmental friendliness, and ease of usage. This approach synthesizes nickel oxide nanoparticles from plant extracts, microorganisms, and other biological products. Phytochemicals from plant extracts, enzymes or proteins from microorganisms, and other biological substances reduce, stabilize, and cap nickel oxide nanoscale material to make it biologically active and compatible.[6,11,12]

The formation of Ag NP requires the reduction of the environmental concentration of Ag^{+} ions to Ag^{0}, which can only be achieved by removing phytochemicals from plants.[13–15] Along with their strong electrical conductivity, chemical stability, and catalytic capabilities, silver nanoparticles (Ag NP) effectively reduce the number of bacteria present. Ag NP is used in research to improve the efficacy of antibiotics because of its capability to remove bacteria and viruses that have developed resistance to antibiotics.[16,17] In recent years, nanoparticles have emerged as valuable agents in several industries, including food and textile, smart agriculture, and waste-water treatment.[18–21]

These nanoparticles have shown potential applications as antiviral, antibacterial, antioxidant, cytotoxic, antitumor, anti-inflammatory, antidiabetic, and bioremediation agents.[2,6,14,22–26] In recent years, microbial infections have become resistant to even the best therapies. This has raised global mortality and morbidity and burdened the healthcare system. Antibiotic use and the development process for antibiotic research have generated concerns, requiring fast action to stop this threat. Fighting antibiotic resistance and other methods for producing new drugs are reviving the toolkit.[15,27]

Phytonanoparticles can function as carrier entities, facilitating the distribution to cells for diverse objectives. Moreover, nanoparticles have a substantial surface area and possess favorable conductivity. The use of phytonanoparticles has played a significant role in advancing novel methodologies within the domains of biomedicine and pharmacology. These advancements include diagnostic and therapeutic techniques, as well as the manufacturing of intelligent pharmaceutical agents.[28–30] The synthesis of metallic silver nanoparticles by the use of *A. officinalis* aqueous leaf extract is the primary purpose of this study endeavor. The use of extract from the leaves, made possible by the abundance of A. O. leaves, offers a simple and affordable method for producing metallic nanoparticles.

Anchusa officinalis L. is an annual or biennial herbaceous plant from the Boraginaceae family. This species may be found in its natural habitat from Europe to the Caucasus.[31] It is a perennial plant that is predominantly found in the biome known as temperate. Internally, they are used to cure coughs and bronchial catarrh, and topically, they are used to heal wounds such as cuts, bruises, and phlebitis. The plant is used in the production of homeopathic medicine. Moreover *A. officinalis* is a non-endemic medicinal plant that is widely distributed and does not require extra conditions to grow. For this reason, it can be considered as a material suitable for widespread use.[32–34]

This study involved the synthesis of silver nanoparticles utilizing the aqueous leaf extract of *A. officinalis*, a plant recognized for its rich chemical composition, medicinal properties and application in traditional medicine. The antibacterial and cytotoxic effects were evaluated to establish a low-cost biomedical agent alternative suitable for low-dose applications, potentially replacing medical drugs that exhibit toxicity at elevated doses for therapeutic use. Synthesis, characterization and biomedical application steps of biogenic AO-AgNPs produced using *A. officinalis* leaf extract are summarized in Figure 1.

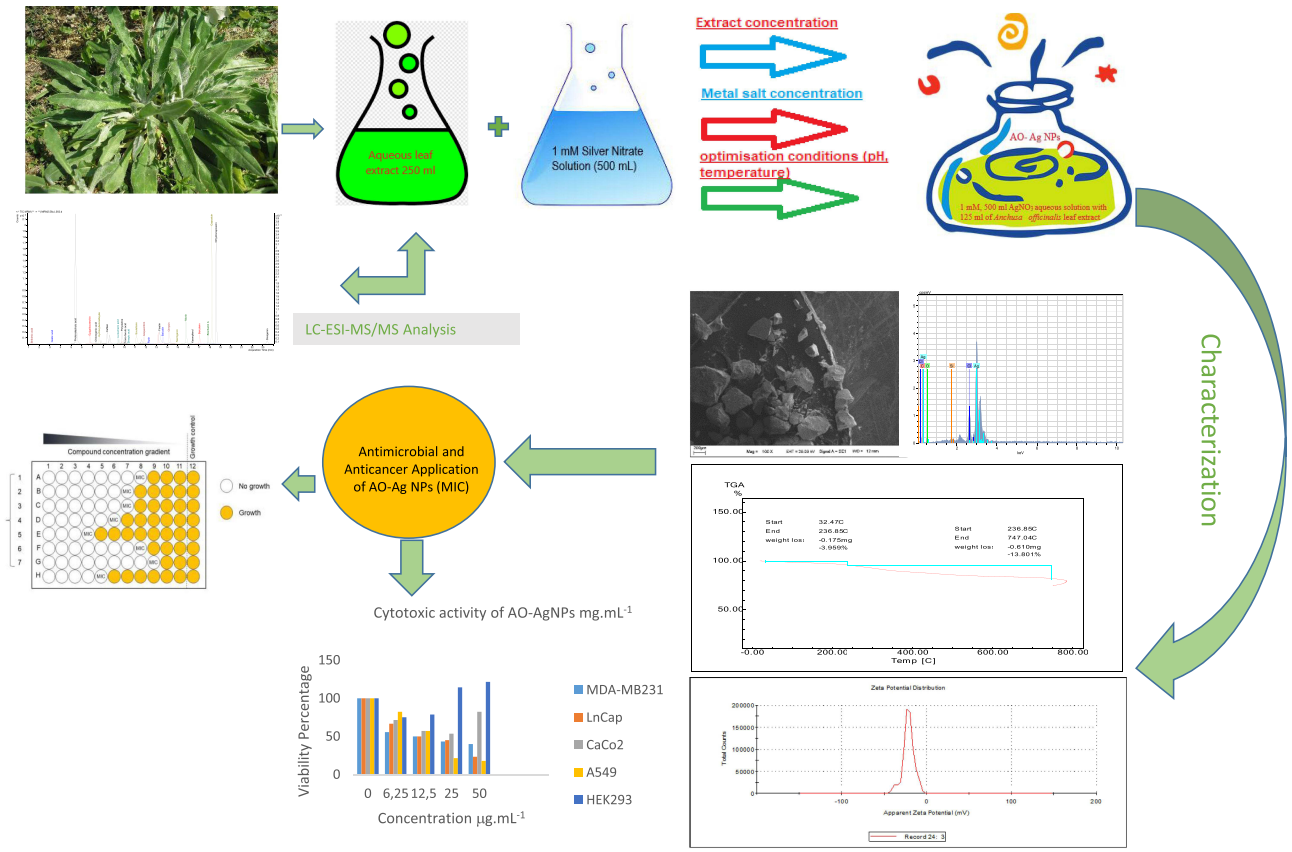

Figure 1 A schematic diagram of the biogenic Ag NP synthesis steps, characterization, and antimicrobial applications.

Experimental Section

Plant Materials and Reagents

The *Anchusa officinalis* leaves that were utilized in this investigation were collected in September from the Mardin Artuklu University Campus (Figure 2). Dr. Cumali Keskin from Mardin Artuklu University verified the taxonomic

Figure 2 Places where *Anchusa officinalis* plant samples were collected (collections).

https://doi.org/10.2147/IJN.S511217

identity of the plant sample. Plant samples were kept in the same institution's Herbarium (voucher no. MAU: 2022–27). The analytical grade phenolic standards, formic acid, ammonium formate, and liquid chromatography grade acetonitrile and methanol were procured from Merck (Germany). Solid silver nitrate ($AgNO_3$, purity 99%; Merck) and antibiotics (vancomycin, fluconazole, and colistin) were employed in the synthesis phase. The antibiotics given in the study were some of the antibiotics used commercially to treat the tested microorganisms. All cell lines were purchased from the European collection of cell cultures (ECACCCC, UK). MTT assays for cell culture were performed at the Biology Research Laboratory of Pamukkale University.

Preparation of Plant Extract

The leaves of *Anchusa officinalis* were collected and then washed under running water to remove any impurities. After this, they went through a process of natural drying at room temperature while being contained in a covered setting. The powder was made from the dried leaves. Weighing the ground samples brought the total to 25 grams, which were then boiled at 85 °C for 20 minutes in a total volume of 250 milliliters of distilled water. Following the completion of the extraction procedure, the formation of color was seen, and then the solution was allowed to gradually return to the temperature of 25 °C, which is considered normal. Following filtration using Whatman No. 1 filter paper, the plant extract was obtained. The resulting extract was stored at a temperature of 4 °C so that it could be used later on in the process of characterizing the compound and conducting research on its biological activity.

Preparation of Silver Nitrate Solution ($AgNO_3$)

After measuring and weighing 0.85 grams of solid $AgNO_3$ (Alpha-Easier) with an analytical purity of 99.8%, a solution of 1 mM silver nitrate was made by dissolving it in 500 milliliters of water.

Green Synthesis of Silver Nanoparticles

AO-Ag nanoparticles were produced by mixing 1 mM of 500 mL aqueous silver nitrate solution with 125 mL of *A. officinalis* leaf extract (4:1 ratio). The pH was adjusted to 8 to enhance the reduction process and inhibit nanoparticle aggregation. Observations were carried out over time for the mixture kept on a stable surface at 22–25°C. After 30 minutes of Ag^+ ions being reduced to Ag^0, the solution lost its transparency and turned dark brown. The maximum absorbance of biologically synthesized AgNPs was determined by wavelength scanning (UV-vis spectroscopy) at various time intervals (10, 15, 20, 25, and 30 minutes) depending on the color change. The main purpose of time-dependent UV-vis spectrometry measurements is to verify the synthesis of AO-Ag NPs. The fact that the absorbances measured at different time intervals give the same result each time is an expression of the synthesis and the stability of the structure. At the end of the synthesis, the solution, which acquired a dark color depending on time, was subjected to centrifugation (in 50 mL Falcon tubes at 15,000 rpm, 5 minutes). The upper liquid portion was extracted. Distilled water was introduced to the sediment at the bottom and subsequently centrifuged again. The procedure was reiterated until the plant extract residues were entirely eliminated from the bottom sediment. The produced AO-Ag nanoparticles were dehydrated in an oven at 65 °C for 48 hours to maintain their suitability for subsequent evaluation. Subsequent to the drying step, the AO-Ag NPs were thoroughly pulverized using an agate mortar and prepared for utilization in the investigation.[35]

LC-ESI-MS/MS Analysis for the Determination of Chemical Composition

To identify the agents involved in bioreduction, the phytochemical composition of the extracted material was characterized using liquid chromatography-mass spectrometry (LC-MS/MS) and Fourier-transform infrared (FTIR) spectroscopy instruments. The findings were utilized as well in the determination of the chemical ingredients of the extract. A dry plant extract weighing 200 mg was combined with 20 mL of methanol, and then, the resulting solution was further diluted to a concentration of 1 mg/mL using a mixture of 50% methanol and high-purity water. Then, the solution underwent filtration using a microfilter and was then transferred to a vial in preparation for LC-ESI/MS/MS analysis. The separation of components was achieved by the employment of a Poroshell 120 EC-C18 column with dimensions of 100 mm length, 4.6 mm inner diameter, and 2.7 mm particle size. The plant mixture that had been filtered was subjected to column chromatography utilizing a carrier phase of 0.1% formic acid and a mobile phase containing 5 mM ammonium formate.

Additionally, mobile phase B, which included 0.1% formic acid in methanol and 5 mM ammonium formate, was also used.[36] The carrier phase facilitates the solubilization of analytes. This is essential for the introduction of analytes into the column, particularly in intricate matrices (eg biological specimens). The solubilization of analytes mitigates column obstruction and facilitates more effective analyte separation. Also the carrier phase is essential for the transport, separation, ionization, and detection of analytes in LC-MS/MS. The appropriate choice of carrier phase facilitates enhanced sensitivity and precision in the detection of analytes.

Characterization of Biogenic AO-Ag NPs

To capture the surface Plasmon resonance (SPR) peaks of the biosynthesized AO-Ag NPs, an ultraviolet-visible spectroscopy (Shimadzu UV-1601) study was carried out. The morphology and elemental mapping of AO-Ag NPs were observed using a scanning electron microscope with energy-dispersive X-rays (SEM-EDX; EVO 40 LEQ, Germany), and TEM analysis. The surface charge and colloidal stability of AO-Ag NPs were assessed using a zeta-sizer device (Malvern). Differential thermal analysis (DTA) and thermo-gravimetric analysis (TGA) were used to measure the thermal stability and weight loss of AO-Ag NPs. Using XRD equipment (X-ray diffractometer RadB-DMAX 11), the crystalline character of AO-Ag NPs was established. Using Fourier transform infrared spectroscopy (Perkin Elmer One, USA), the functional groups involved in the bioreduction of AO-Ag NPs were identified. These groups were generated from plant extracts. The visible light spectrum was captured between 800 cm^{-1} and 4000 cm^{-1}.

The Evaluation of the Antimicrobial Properties of AO-Ag Nanoparticles

The ability of the green synthesized AO-Ag NPs to inhibit the growth of gram (+) bacterial strains (*Staphylococcus aureus* ATCC 29213 and *Bacillus subtilis*) and gram (-) bacterial strains (*E. coli* ATCC 25922 and *Pseudomonas aeruginosa*) as well as *Candida albicans* yeast was used to determine their antimicrobial properties. Pathogenic microbial strains were obtained from the Mardin Artuklu University Research Laboratory. Gram bacteria were inoculated onto nutritional agar, while the yeast *Candida albicans* was cultivated on Sabouraud dextrose agar medium. The samples were then incubated at a temperature of 37 °C in an oven for a duration of one night to facilitate growth. Gram (+) and gram (-) strains were grown in Muller Hinton liquid medium (MHA), whereas *C. albicans* yeast was grown in RPMI liquid medium. The 0.5 Mc Farland standard was used to assess the turbidity of the pathogenic organisms that survived the incubation period.[36] The minimum inhibition concentration (MIC) approach was used to evaluate the inhibitory effects of AO-Ag NPs on the growth of pathogen microorganisms.

Cytotoxic Activity of Biogenic AO-Ag NPs

In order to examine the cytotoxic effects of AO-AgNPs on prostate (LnCap), breast (MDA-MB231), colon (Caco2), and lung (A549) cancerous cells, a healthy human embryonic kidney (HEK293/as a control) cell line was employed. AO-AgNPs were applied to all cell lines at concentrations of 0, 6.25, 1.25, 25 and 50 mg/mL with the MTT assay. The prostate cancer cell line (LnCap) and breast cancer cell line (MDA-MB231) were cultured in RPMI medium supplemented with 10% fetal bovine serum (FBS) and 1% penicillin/streptomycin. The colon cancer cell line (Caco2), lung cancer cell line (A549), and human embryonic kidney cell line (HEK293) were cultured in DMEM medium supplemented with 10% FBS and 1% penicillin/streptomycin. When the cells reached a state of 80–90% confluence, the cells were removed with the help of Trypsin–EDTA. Subsequently, the cells were resuspended in fresh media and quantified using a light microscope aided by trypan blue dye. A total of 1000 cells were placed in each well of 96-well culture plates and kept in a 37°C, 5% CO_2 incubator for 24 hours (pH value adjusted as 7.4). After the 24-hour incubation period, AO-AgNPs were dissolved in dimethyl sulfoxide (DMSO), exposed to different quantities in the cells, and incubated for another 24 hours. After completing the treatment time, 100 µL of media and 10 µL of MTT (3-(4,5-Dimethylthiazol-2-yl)-2,5 Diphenyltetrazolium Bromide) were introduced to the cells and left to incubate for 2–4 hours. The formations that were produced were dissolved using DMSO, and their absorbances at a wavelength of 590 nm were measured using the NanoDrop instrument.[36] The data was read and analyzed using the GraphPad application.

$$\text{Viability of cell lines}(\%) = (\text{Treatment sample absorbance}/\text{Control absorbance}) \times 100$$

Statistical Analysis

GraphPad Prism was used to conduct an unpaired *t*-test as part of a statistical analysis of the collected data. The data were presented as the standard deviation (n = 3) plus or minus the mean. Statistical significance was defined as a p-value of less than 0.05.

Results and Discussion

This article presents a study on the biogenesis of silver nanoparticles using an aqueous extract derived from the leaves of *A. officinalis*. The selection of *A. officinalis* leaf for the current investigation was based on its reported content of flavonoids and phenolic compounds, which are known to contribute to its antibacterial properties.[33] Phenolic compounds and other chemical components found in plant leaf extracts effectively reduce the reactivity of silver salts and show remarkable resistance to the particle aggregation process.[37] The stability of silver nanoparticles can be improved by a process known as coating with groups capable of binding to the bioactive compounds present in the biomaterial, which is preferred for biological synthesis. One of the most important reasons for the selection of A. officinalis plant in the study was its rich biochemical content and easy availability in the research area. Phytochemicals are naturally occurring bioactive substances that are present in a variety of sources such as vegetables, fruits, medicinal plants, fragrant plants, leaves, flowers, and roots. These molecules serve as a defensive mechanism against illnesses. Phytochemicals derived from natural sources include a wide array of chemical entities, including but not limited to polyphenols, flavonoids, steroidal saponins, organosulphur compounds, and vitamins.[38–40]

Plant growth and development may be negatively affected by both biotic and abiotic stressors, leading to nutritional deficits, hormonal imbalances, ion toxicity, as well as osmotic and oxidative stress. The cellular-level biosynthesis of secondary metabolites is considered the most efficacious mechanism for plants to mitigate stress conditions. These metabolites consist of organic compounds that aid in stress reduction by bolstering antioxidant activities, detoxifying harmful ions, regulating nutrient uptake, and facilitating the transport and distribution of various hormones.[41,42]

The current investigation aimed to identify the phytochemical components included in the composition of the leaf extract of *A. officinalis*. The content identification included the analysis of methanol extracts obtained from the plant leaf, which was used in the biosynthesis of silver nanoparticles. This analysis was conducted using LC-MS/MS, and the results are shown in Table 1.

Table 1 The Results of the LC-MS/MS Quantification of the Methanol Extract of Anchusa Officinalis

Standard Compounds	R^2	RT	LOD (μg/mL)	LOQ (μg/mL)	Recovery (%)	Final Con. (μg/g)
Shikimic acid	0.98	1.39	13.1	17.3	99.90	ND
Gallic acid	0.99	2.89	14.3	17.90	100.00	ND
Protocatechuic acid	0.99	5.39	25.8	43.5	100.00	22.82±0.12
Epigallocatechin	0.99	6.61	60.1	83.0	100.00	ND
Chlorogenic acid	0.99	7.35	12.8	17.3	99.80	15.41±0.09
Hydroxybenzaldehyde	0.99	7.61	23.1	39.1	99.50	3.76
Caffeine (Caffeic acid)	0.99	7.80	9.7	11.5	99.90	185.36±0.45
o-coumaric acid	0.99	9.41	33.7	42.3	100.10	9.20±0.07
Resveratrol	0.99	9.57	6.2	8.2	100.20	0.42±0.03
Polydatine	0.99	9.65	12.3	19.5	99.80	ND
Salicylic acid	0.99	9.68	8.4	10.2	99.90	102.51±1.04

(*Continued*)

Table 1 (Continued).

Standard Compounds	R^2	RT	LOD (μg/mL)	LOQ (μg/mL)	Recovery (%)	Final Con. (μg/g)
Trans ferulic acid	0.99	10.12	13.6	17.4	100.10	25.29±0.25
Sinapic acid	0.99	10.41	67.2	84.2	100.00	ND
Scutellarin	0.99	11.13	15.1	20.2	99.70	23.45±0.22
Isoquercetin	0.99	11.87	15.8	22.8	99.80	ND
Rutin	0.99	12.35	16.1	21.1	100.20	6042.17±2.21
Fisetin	0.99	13.33	10.0	12.6	100.00	ND
Baicalin	0.99	13.81	24.4	30.3	99.80	ND
Chrysin	0.99	14.11	0.010	0.010	99.90	ND
Naringenin	0.99	14.85	2.8	4.1	100.00	22.12±0.11
Morin	0.99	15.82	21.2	27.3	99.90	ND
Kaempferol	0.99	16.45	12.4	17.4	99.80	ND
Baicalein	0.99	16.96	24.2	30.1	99.90	ND
Biochanin A	0.99	17.81	214	246	99.90	ND
Capsaicin	0.99	18.11	62.9	81.9	99.90	ND
Dihydrocapsaicin	0.99	18.62	57.2	76.2	100.00	ND
Diosgenin	0.98	23.25	11.5	16.5	99.90	ND

Abbreviations: RT, Retention time (minutes); ND, Not determined; LOD, Limit of detection; LOQ, Limit of quantification; LC-MS/MS, Liquid chromatography-tandem mass spectrometry.

Rutin (Vitamin P) is the most known secondary metabolite, and it has been found in a variety of fruits and fruit rinds, particularly citrus fruits and berries. Vitamin P, commonly known as rutin, is an essential nutrient that may be found in a broad variety of foods, including vegetables, fruits, and medicinal plants like asparagus and buckwheat.[42,43] Rutin has a wide variety of pharmacological activity, including those that are antimicrobial, anticancer, spasmolytic, anti-allergenic, DNA protective, vasoactive, antihyperlipidemic, anti-inflammatory, antiaggregant, and antihypertensive. Due mostly to its low solubility, rutin's poor bioavailability is its primary drawback. Notably, the majority of strategies concentrate on boosting aqueous solubility. A different method of drug delivery has recently been devised to reduce the size of the particles to overcome the poor water solubility of certain medications. A greater dissolution rate, more surface area, and improved saturation solubility are the results of smaller drug particles. To enhance its physicochemical characteristics, rutin must be formulated into drug nanocrystals. As a result, nanomaterials made from plant extracts with a high rutin content boost biological activity.[43–45]

Classified as hydroxycinnamic acid, caffeine is a plant-derived substance that has both acrylic and phenolic functional groups. As an alternate tactic to fight microbial pathogenesis and chronic infections brought on by bacteria, fungi, and viruses, caffeic acid has been widely used. Caffeic acid (CA), a bioactive molecule, has anti-oxidant properties and may treat and prevent inflammatory and cancerous disorders. Anti-oxidant, anti-viral, anti-inflammatory, and anti-cancer effects have been attributed to CA as well as its derivatives. Due to its pro- and anti-oxidant qualities, caffeic acid fights cancer. In a similar vein, many caffeic acid derivatives, including sugar esters, organic esters, glycosides, and amides, have been discovered naturally or chemically as possible antibacterial agents. Caffeic acid and its derivatives have been used in nanoformulation or in conjugation with other bioactive compounds to address the problems of poor stability and water insolubility.[46–51]

Salicylic acid (SA) is classified as a crystalline organic carboxylic acid, exhibiting solubility in alcohol and limited solubility in water. Salicylic acid is a quite potent irritant that should not be applied to sensitive skin. Its low water solubility restricts the amount that can be added to formulations, which leads to poor bioavailability and transdermal activity. It can boost biological activity since salicylic acid-containing nanoformulations no longer have issues with low stability and water insolubility.[52] SA is a phenolic derivative that is widely distributed in the kingdom of plants. Salicylic acid (SA) is a phenolic molecule that is found in a variety of plants, where it plays a crucial function in protecting against pathogenic microorganisms,[53] The inhibitory effect on prostaglandin production is largely responsible for the majority of the pharmacological effects shown by salicylic acid.[54]

The COVID-19 pandemic brought attention to the urgent need to gain a deeper understanding of the significance of SA in mitigating illness development and ameliorating symptoms. The assessment of the role of acetylsalicylic acid as an antiviral agent and potential co-treatment for Coronavirus disease 2019 (COVID-19) has been significant due to the observed decrease in mortality risk associated with the use of aspirin in patients affected by COVID-19.[55,56] In this study, 27 standard compounds were used as a reference for analysis (Figure 3). The chromatogram was utilized as a means of evaluating the samples. It was determined that out of the 27 standard compounds examined, 11 of them (Protocatechuic acid, chlorogenic acid, caffeic acid, o-coumaric acid, resveratrol, salicylic acid, trans ferulic acid, scutellarin, rutin, and naringenin) were present in the plant extracts. Among the phenolic structures that were identifiable, resveratrol was found to have the lowest quantity at 1.63±0.03 mg/g. The plant's structure included a significant number of chemicals, with rutin (6042.17±2.21), caffeic acid (185.36±0.45), and salicylic acid (102.51±1.04) being the most abundant. It is possible to say that the current abundant phenolic content performs the function of a reducing agent in the process of the synthesis of nanoparticles and plays an active role in the antibacterial properties of the nanoparticles that have been created.

Characterization

Monitoring the Formation of Silver Nanoparticles Macroscopically and with UV-Vis Spectroscopy

The spectrophotometer (Shimadzu; UV-1601) was used to measure the ultraviolet-visible (UV-vis) spectra of the AgNPs that were generated and purified. The observations were performed over the wavelength spectrum from 300 to 800 nm.

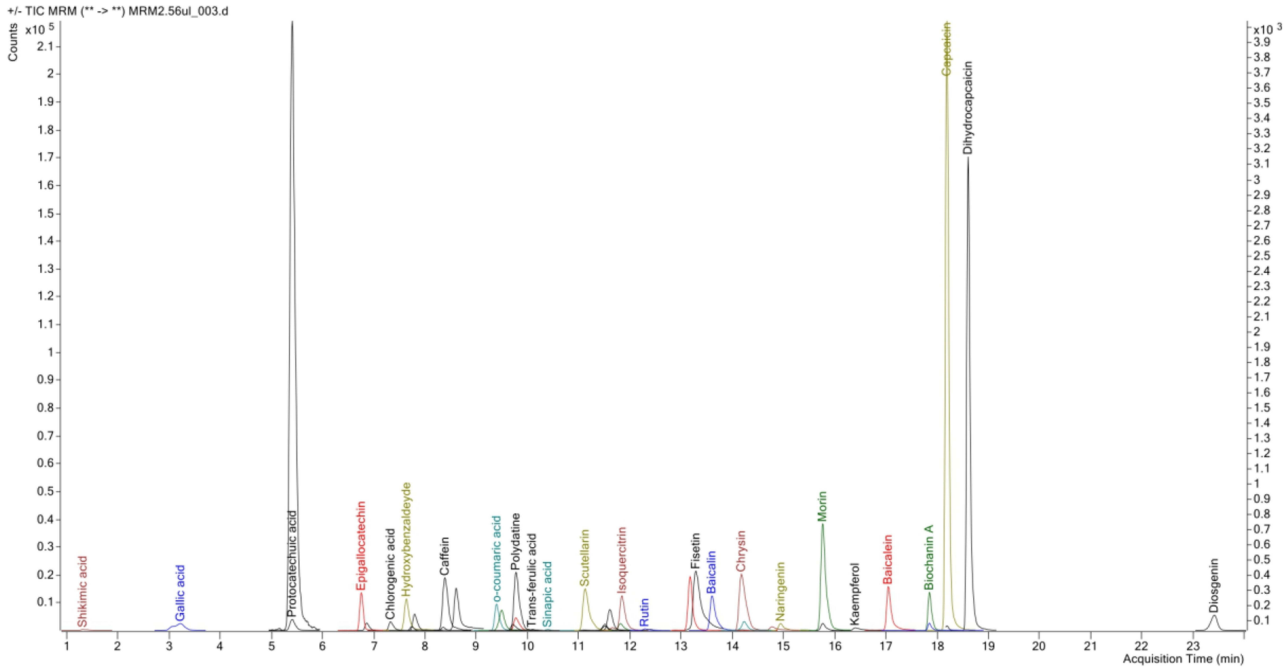

Figure 3 LC-ESI-MS/MS analysis chromatogram of *Anchusa officinalis* extract.

The reaction between the silver nitrate solution and the plant extract led to a rapid alteration in the color of the solution, transitioning from a pale brown shade to a deep brown shade. The presence of silver nanoparticles was then seen in samples examined at regular intervals of 10, 15, 20, 25, and 30 minutes. A maximum absorbance band was observed at 466 nm, confirming Ag NPs' formation (Figure 4). These results were similar to those reported in the literature.[35,36]

UV-visible spectroscopy is a vital method used to understand the production process of silver nanoparticles during the early synthesis phase. The surface plasmon resonance of silver nanoparticles is significantly influenced by their morphology, dimensions, and dispersion, resulting in unique characteristics. Silver nanoparticles of diminutive size and spherical morphology exhibit absorption between 400 and 500 nm, distinguished by sharp peaks. Larger silver nanoparticles exhibit a redshift effect by absorbing at longer wavelengths and displaying bigger peaks. The observed phenomena also indicate the stability of silver nanoparticles (Ag NPs). This phenomenon may be ascribed to particle aggregation resulting from the reduction in peak strength and the widening of peaks, followed by the appearance of secondary peaks at longer wavelengths. The highest absorbance value recorded at 466 nm over various time periods demonstrated that aggregation did not transpire, confirming the stability of the synthesized silver nanoparticles' structure.[35,36,57]

FTIR Spectrum Data Analysis

Fourier Transform Infrared (FTIR) spectroscopy analyses were conducted to identify the potential functional groups in biomolecules found in the plant extract that were responsible for reducing silver ions into Ag NPs. Absorption bands centered at 3300–3900 cm^{-1}, 2940 cm^{-1}, 1600–1700 cm^{-1}, 1350–1450 cm^{-1}, and 1000–1100 cm^{-1} are associated with aromatic compound O–H and C–H stretching, carbonyl compound C=O stretching, C–C, C–O–C, C–N, and C–O bonds, amide N–H stretch vibration, and C=C groups. Phytochemicals such as polyphenols, proteins, alcohols, terpenoids, enzymes, and alkaloids serve as accessible sources of these connections. Thus, data suggests that water-soluble secondary plant metabolites, such as flavonoids, may potentially encapsulate silver nanoparticles. Silver nanoparticles, classified as heavy metals, adhere to microbial proteins and bind to their thiol groups, resulting in the inactivation of these proteins. The dimensions of silver nanoparticles are a critical element influencing their efficacy against germs. This occurs because smaller particles possess a greater surface area, enhancing their adhesion to bacterial cell walls, hence obstructing the cell's infiltration and respiration processes. The Fourier Transform Infrared (FTIR) spectrum of aqueous extracts from *A. officinalis* leaves (Figure 5A) exhibited prominent peaks at wavenumbers of 3902, 3853, and 3735 cm^{-1}, corresponding to the stretching vibrations of phenolic hydroxyl (OH) groups.[35,58–60] Another notable peak was observed at 3317 cm^{-1}, which can be attributed to the stretching vibrations of hydroxyl (–OH) groups. Additionally, several peaks were observed at wavenumbers 2377, 2310, 2251, 2130, and 1992 cm^{-1}, indicating the presence of N-C aromatic and aliphatic amines

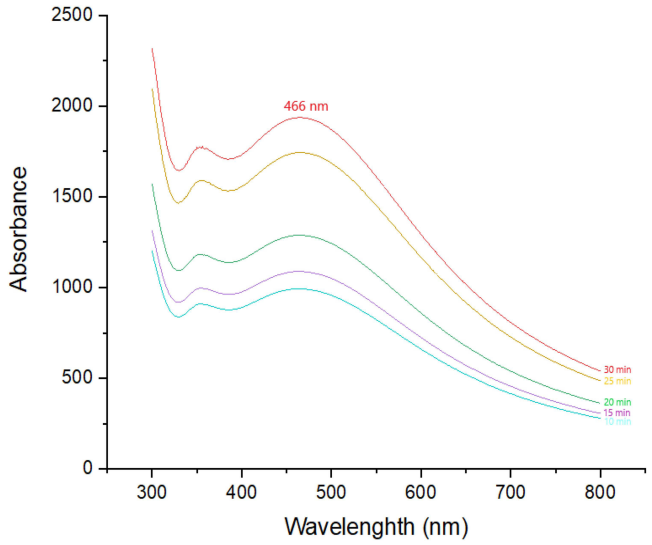

Figure 4 The ultraviolet-visible (UV-vis) spectrum of silver nanoparticles that were produced using *A. officinalis*.

https://doi.org/10.2147/IJN.S511217

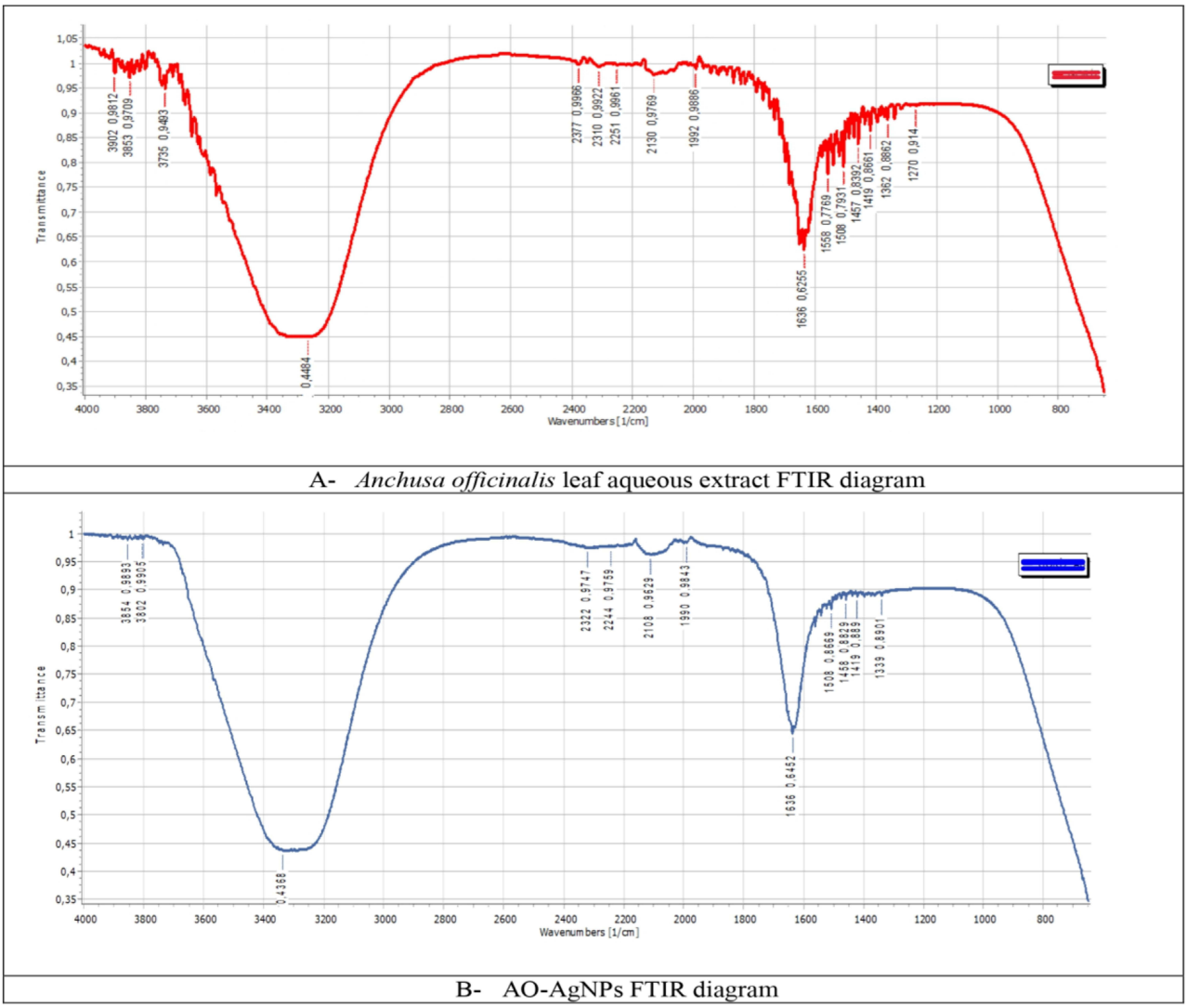

Figure 5 FTIR spectra of pure AO leaf aqueous extract (**A**) and AO-capped Ag NPs (**B**).

or C–C bonds within the aromatic ring structure. The peak at 1636 cm^{-1} can be attributed to the amide I bond of proteins, specifically the stretching of carbonyl groups in proteins. Furthermore, peaks at 1558 and 1508 cm^{-1} indicate stretching vibrations of the aromatic ring structure. Symmetrical stretching of the carboxylate group was observed at wavenumbers 1457 and 1419 cm^{-1}. The peak at 1362 cm^{-1} suggests the presence of C–C bonds within the aromatic ring or amide group II. Lastly, the peak at 1270 cm^{-1} corresponds to the stretching vibrations of aromatic secondary amine (C-N) groups.[39,61,62] However, the creation of AO-Ag NPs resulted in shifts of peaks, specifically at 3854 and 3802 to 3339 cm^{-1}, 2322, 2244, 2108 to 1990 cm^{-1}, 1636 cm^{-1}, 1508, 1458, 1419 to 1339 cm^{-1} (Figure 5B). Plant extracts often contain polyphenols, flavonoids, and other reducing agents that convert Ag^{+} to Ag° (metallic silver). These functional groups change vibrational frequencies and FTIR peaks after reduction. The interaction between plant extract and silver ions creates new or broken hydrogen bonds, which may change the FTIR spectrum. Peaks disappear when functional groups are fully engaged in stability or decrease. The development of new complexes or bonds between the plant extract and silver ions may be indicated by the emergence of new peaks. These shifts indicate the reduction of the respective functional groups. The data obtained indicate that the polyphenols included in the aqueous leaf extract of *A. officinalis* exhibit C–C and C-N vibration stretch in AO-Ag NPs, suggesting their potential role as capping and stabilizing factors in the production of these nanoparticles.[58,59] The functional groups that may be responsible for the reduction of silver nitrate and some of their functions were summarized in Table 2.

Table 2 The Functional Groups Potentially Involved In the Reduction of Silver Nitrate and Their Associated Functions

Functional Structure	Group/Bound/ Stretching	Their Importance for Reaction	Ref.
Alkenes	C=C Groups	Polymerization and reactivity in addition to reactions	[35]
Alcohols, ethers, esters, carboxylic acids	C–O Bonds	As well as reactivity in hydrolysis and reduction, polarity	[59,60]
The fundamental structure of organic compounds	C–C Bonds	Double and triple bonds exhibit both stability and reactivity.	[35,61]
Amines, amides, nitriles	C–N Bonds	Hydrolysis, basicity, and reactivity in nucleophilic substitution	[60,61]
Amides	Amide N–H Stretching	The process of hydrolysis involves hydrogen bonding and reactivity.	[60,62]
Carbonyl group in aldehydes, ketones, carboxylic acids, esters, amides	C=O Stretching	In nucleophilic addition, reduction, and condensation, polarity, reactivity, and condensation	[35,59]
Chemicals such as carboxylic acids, alcohols, and phenols include the hydroxyl group.	O–H Stretching	Chemical reactions involving hydrogen bonds, esterification, dehydration, and oxidation	[39,59,60,62]
Structures composed of hydrocarbons and organic compounds	C–H Stretching	Integrity of the structure, reactivity in substitution, elimination, and oxidation interactions	[59]

XRD Data Analysis of AO-Ag NPs

The crystalline structures of silver nanoparticles (JCPDS No 65-2871) were examined using the X-ray diffractometer (RadBDMAX II), which is computer-controlled. The analysis was conducted within the angular range of $3°\leq 2\theta \geq 80°$. The determination of the crystal size of silver nanoparticles was performed utilizing the Debye-Scherrer equation. The equation (1) can be expressed as $D = K\lambda/(\beta \cos\theta)$.[60] The equation represents many parameters related to a particle, where D represents the crystal diameter of the particle in nanometers, K denotes a constant with a value of 0.90, λ represents the wavelength of X-ray in angstroms (Å), β signifies the breadth of the greatest peak at half height in radians, and Q represents the Bragg angle in degrees. Ibrahim et al, reported that in the AgNPs biosynthesis study using A. graecorum plant extract, the crystalline silver planes (101), (111), (200), (220) and (311) showed strong diffraction peaks at 28.81°, 31.98°, 37.85°, 46.03° and 77.06°.[61] According to XRD data of the El Megdar et al, silver nanoparticles exhibited a cubic crystal structure at 2θ angles. With discernible peaks at 111, 200, 220, and 311°, the values of these peaks were as 38.21°, 44.29°, 64.55°, and 77.44°.[62] Said et al, reported that the average crystallite sizes ranged from 28 to 60 nm according to the peaks corresponding to Bragg diffraction for the silver nanocrystal they synthesized using *Lawsonia inermis* extract.[63] The study revealed that the silver nanoparticles exhibited a cubic crystal structure, as evidenced by the reflection values of 38.12, 44.20, 64.58, and 77.4 in the (111), (200), and (311) layers, respectively (Figure 6). Upon analysis of the X-ray diffraction (XRD) data, the Debye-Sherer equation was employed to determine the average size of the nanoparticles, yielding a value of 27.06 nm. It was seen that the data obtained were compatible with previous studies.

SEM-EDX and TEM Analysis of Biogenic Silver Nanoparticles

To get a comprehensive knowledge of the characteristics of AgNPs synthesized using biological materials, it is essential to acquire information on the surface morphology and topography of the sample. A fundamental characteristic of nanoparticles (NPs) is their size, which may be classified as either nano or micro. Electron microscopy is often used to ascertain the dimensions and distribution of particles. Laser diffraction techniques are used to evaluate raw materials in the solid phase, while SEM or TEM images are utilized to determine the dimensions of individual particles and aggregates.[60] The scanning electron microscope (SEM) was used to assess the surface shape, dimensions, aggregation, and dispersion of the nanoparticles for imaging (Figure 7A–C). The analysis indicated that under specific conditions, the AgNPs exhibited a spherical morphology. The scanning electron microscopy (SEM) images further revealed that the generated silver nanoparticles (Ag NPs) exhibit a non-agglomerated particle morphology. With a size range of 8.5 to 40.2 nm and an average particle size of 28.5 nm, the TEM images of the AO-AgNPs showed that the nanoparticles were

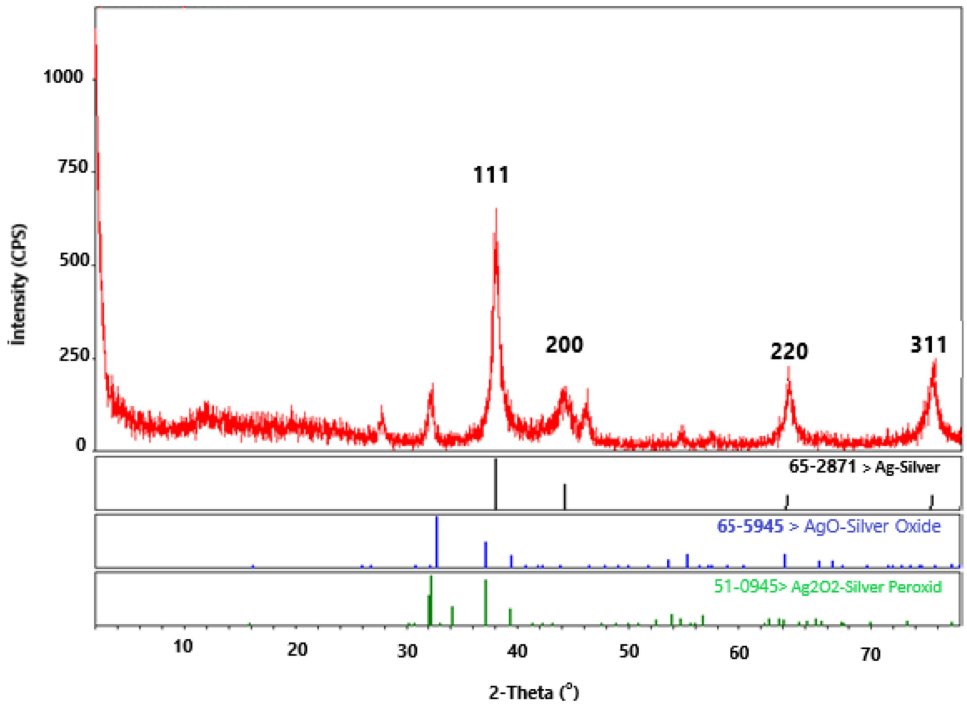

Figure 6 XRD diagrams of biosynthesized AO-Ag.

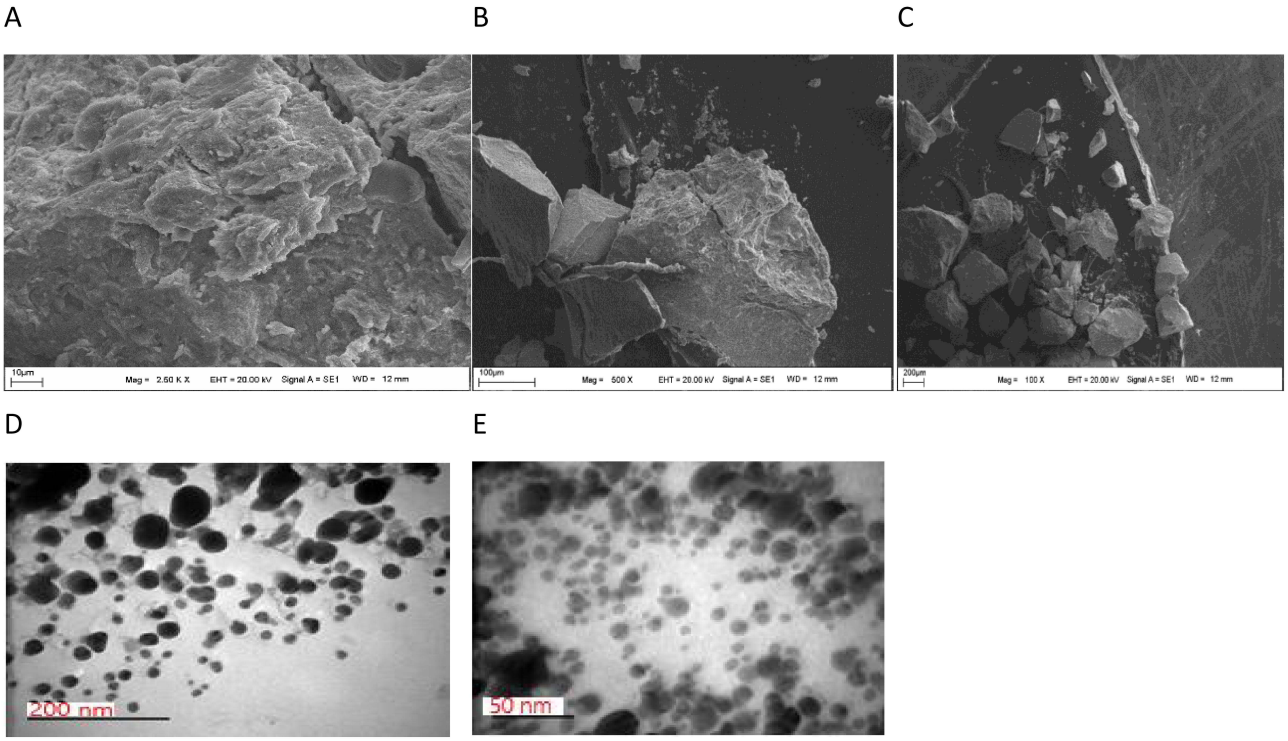

Figure 7 Different magnifications SEM (**A**–**C**), and TEM (**D**–**E**) images of biologically synthesized silver nanoparticles by *Anchusa officinalis* leaf aqueous extract.

spherical in form and about the same size as the NPs determined from the XRD result (Figure 7D and E). Because of their enhanced surface reactivity, ROS production, and cellular absorption, smaller nanoparticles often exhibit stronger antibacterial and cytotoxic properties. The TEM images revealed the previously described aggregation of small particles and scattered nanoparticles with metallic silver's face-centered cubic (fcc) crystalline structure.[35,36,64]

Energy distribution spectra of the obtained Ag NPs and EDX analysis results show that the silver particles were smaller than 100 nm and the elemental composition mostly belongs to silver in the EDX analysis. The EDX spectrum obtained from the produced silver nanoparticles exhibited a prominent peak at around 3 keV, indicating that elemental silver constituted a significant proportion of the nanoparticles. Additionally, there were observations of faint signals originating from C and O at energy levels of 0.2 and 0.5 keV, respectively.

The observed signals could perhaps be attributed to the biomolecules employed for capping during sample loading, as well as the presence of phytochemicals responsible for facilitating the reduction reactions (Figure 8). In addition, it can be asserted that the Si signal observed at 1.7 keV is derived from the glass material employed in the grinding process of the nanomaterial, while the Cl signal was attributed to the water utilized during the synthesis phase. Silver had the greatest perfect peak among the elements, that the produced silver nanoparticles were pure.

TGA-DTA Analysis Result of Biogenic Ag NPs

The degradation temperatures of silver nanoparticles that were generated using *Anchusa officinalis* leaf extract were assessed using TGA-DTA analysis (Shimadzu TGA-50 instrument). Thermogravimetric analysis (TGA) is a highly efficient analytical technique utilized to quantify alterations in the mass of a specimen over a given duration while

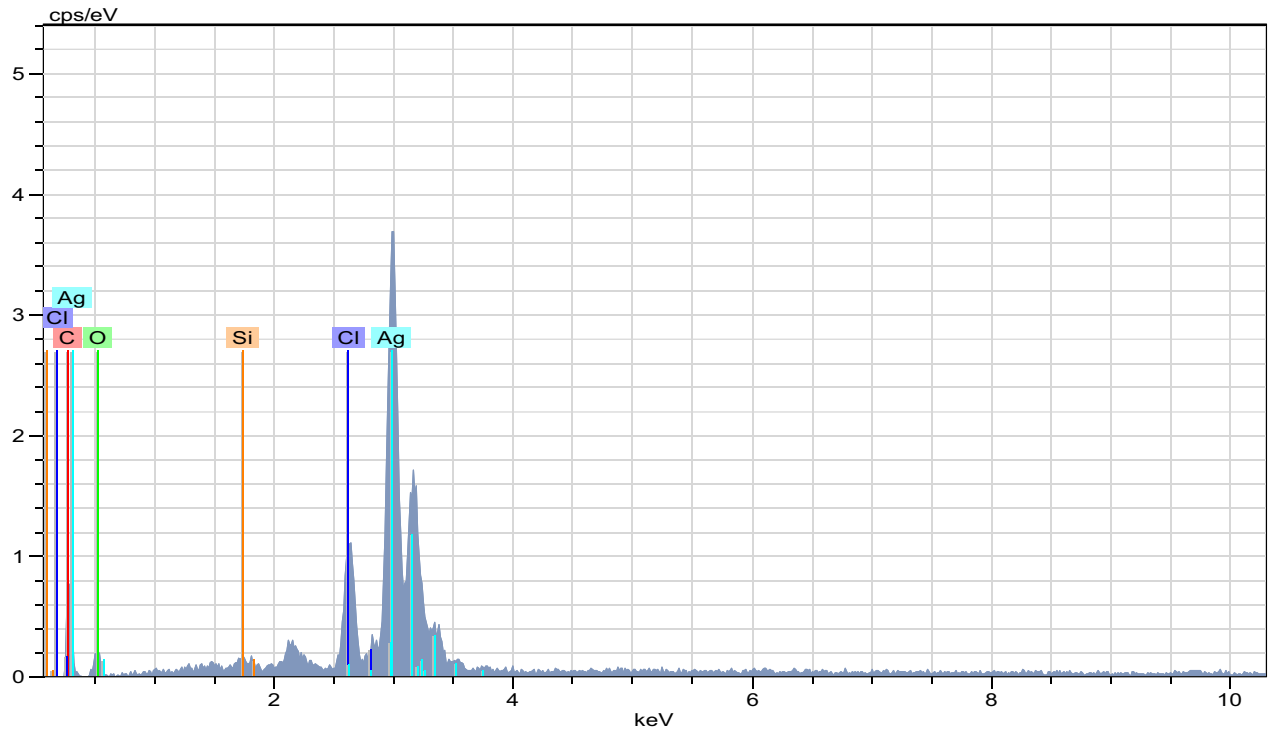

El AN	Series	unn. [wt.-%]	C norm. [wt.-%]	C Atom. [at.-%]	C Error [%]
Ag 47	L-series	55.24	74.73	28.60	3.2
C 6	K-series	8.37	11.32	38.91	2.7
Cl 17	K-series	1.78	2.41	2.81	0.5
Si 14	K-series	0.05	0.06	0.10	0.0
O 8	K-series	8.47	11.46	29.58	
	Total:	73.91	100.00	100.00	

Figure 8 EDX data of AgNPs synthesized with leaf extract of *Anchusa officinalis* plant.

https://doi.org/10.2147/IJN.S511217

subjecting it to varying temperatures in a controlled environment.[64] The utilization of DTA analysis provides a more comprehensive understanding of the thermal stability characteristics shown by various materials. Differential thermal analysis (DTA) is a commonly employed technique in the field of thermal analysis to quantify the energy variations that arise from either a state change or a chemical reaction.

The differential thermal analysis (DTA) technique relies on the measurement of the temperature disparity between the sample being analyzed and a reference material while subjecting them to controlled heating or cooling conditions.[65] The experimental parameters for thermal gravimetric analysis were settled at a temperature range of 30–900 °C, a heating rate of 10 °C, and a flow rate of 20 mL/min. The analysis was conducted under a nitrogen gas atmosphere. The gained results were shown on a graph (Figure 9).

The thermogravimetric analysis (TGA) curve illustrates the reduction in sample mass resulting from thermal deterioration. The observed mass loss of 3.959% for the acquired AO-Ag NPs within the temperature range of 32.17–236 °C can be attributed to the presence of moisture. Similarly, the mass loss of 13.801% within the temperature range of 236.85–747 °C can be attributed to the degradation of the cellulosic material. The data presented in Figure 9 indicates

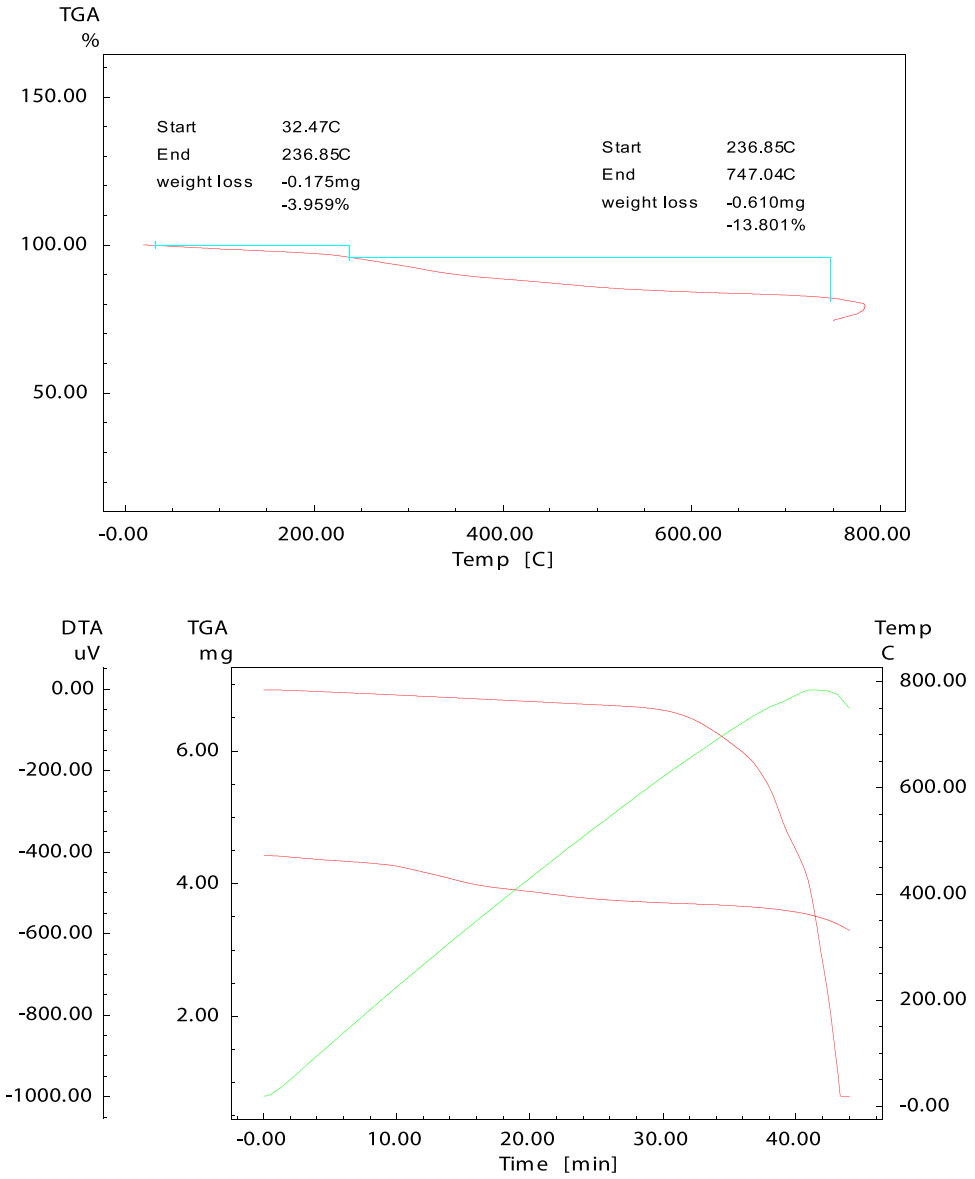

Figure 9 The results of the TGA-DTA study obtained from biogenic silver nanoparticles.

that around 14% of the synthesized material experiences degradation when exposed to temperatures of up to 750 °C. This observation suggests that the synthesized nanoparticle exhibits a notable degree of stability and resilience towards elevated temperatures.

Zeta Potential Analysis of AO-Ag NPs

The existence of zeta potential is a characteristic physical property that can be observed in particles suspended in a medium, macromolecules, or the surfaces of materials. Silver nanoparticles (AgNPs) with a negative zeta potential have greater inhibitory effects on Gram-negative bacteria compared to Gram-positive bacteria. The primary distinction between these two bacteria lies in their cell wall architectures: The outer membrane of Gram-negative bacteria consists of lipopolysaccharides and a thin coating of peptidoglycan. The negative zeta potential of AgNPs interacts more effectively with negatively charged LPS, resulting in membrane rupture, increased permeability, and cell death. The structural complexity of Gram-negative bacteria's outer membrane renders it more susceptible to AgNP damage. Gram-positive bacteria lack outer membranes and possess thick peptidoglycan layers. Gram-positive bacteria have greater resistance to negatively charged zeta potential silver nanoparticles owing to their robust peptidoglycan layer.[66,67] The zeta potential analysis was conducted to ascertain the surface charges of the produced AgNPs, yielding a value of −21.2 mV (Figure 10). The negative charge distribution of AgNPs is of significant importance. The observation that the acquired AgNPs possess a solely negative charge suggests the absence of aggregation or grounding, hence indicating their stability.

Antimicrobial Assay Results

Although the precise mechanism is unclear, Ag NPs may stop bacteria from growing by releasing Ag ions. This is mostly because AgNPs have the ability to release a significant amount of reactive oxygen species (ROS), which may damage cell membranes and eventually lead to cell death. More precisely, AgNPs are easily oxidized by other molecules, including oxygen, producing Ag^{+} in the process. Oxidative stress may be triggered in part by excessive reactive oxygen species (ROS) levels. Endoplasmic reticulum stress is known to be a crucial protective mechanism in addition to being a cell signal transduction system. According to earlier research, the partial breakdown of the bacterial cell wall brought on by charge interactions between the positively charged silver nanomaterial and the negatively charged cell wall is what gives NPs their antibacterial qualities. Additionally, it has been shown that the interaction of silver nanoparticles with sulfur or phosphorylated proteins found in bacterial cell walls destabilizes and depolarizes the bacterial cell membrane, compromising membrane integrity and H+ leakage.[36,68,69] Ag ions stick to cell walls and cytoplasmic membranes due to electrostatic attraction and sulfur protein affinity. Adhered ions increase cytoplasmic membrane permeability and upset the bacterial envelope. After cells absorb free Ag ions, respiratory enzymes deactivate, generating reactive oxygen species but halting adenosine triphosphate synthesis. Oxidative stress can damage cell membranes and modify DNA. As

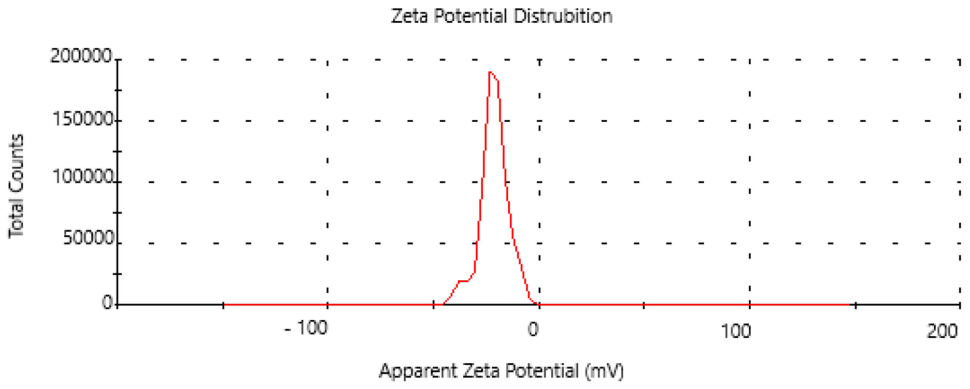

Figure 10 Zeta potential analysis of AgNPs obtained from the leaves of the *Anchusa officinalis* plant.

https://doi.org/10.2147/IJN.S511217

DNA contains sulfur and phosphorus, silver ions can interfere with DNA replication and cell reproduction or kill microbes. Silver also denatures cytoplasmic ribosomes, inhibiting protein synthesis. Ag-NPs are responsible for the production of silver metal ions, which play a significant role in the modification of the structure of the membranes of bacteria. This, in turn, causes the permeability of the bacteria's membranes to rise, which finally results in the death of the living cells. When Ag+ ions are released from Ag-NPs, they have the potential to cause damage to biological macromolecules such as phospholipids, proteins, and nucleic acids. This may result in an increase in the antibacterial effectiveness of Ag-NPs. The electrostatic contact between the positive charge of Ag+ ions and the negative charge of the bacterial cell wall is likely the cause of the creation of gaps or holes in the bacterial membrane or cell wall. This interaction is likely to be induced by the presence of Ag+ ions.[32,38,65,66,70,71]

Aqueous extracts of *A. officinalis* leaves were used to create AO-Ag nanoparticles, and their antibacterial efficacy was the focus of this investigation. Antimicrobial effectiveness against various bacterial strains was assessed in the study using the minimum inhibition concentration method. These strains included gram-positive bacteria like *B. subtilis* and *S. aureus*, gram-negative bacteria like *P. aeruginosa* and *E. coli*, and the yeast strain *C. albicans*. The experimental setup included the use of water as a negative control, while vancomycin (128 mg/mL), colistin (128 mg/mL), and fluconazole (128 mg/mL) were employed as positive controls. The growth inhibitory effects of AO-Ag nanoparticles were seen against all gram-positive and gram-negative bacterial strains, as well as yeast, as shown in Table 3. The antibacterial properties of silver nanoparticles are subject to several influencing parameters, including zeta potential, dimensions, form, colloidal state, pH value, temperature, dosage, and the specific microbial strains involved.

The zeta potential of silver nanoparticles is a basic characteristic that governs their electrostatic interactions with bacterial surfaces. The decreased susceptibility that includes bacterial species to AO-Ag NPs may be ascribed to the negatively charged nature of the nanoparticles' surface, leading to a reduced probability of electrostatic adherence to the bacterial surface. The presence of surface-active chemicals with negative charges on the surface of AO-Ag NPs, as suggested by a zeta potential value of −21.2 mv, may provide a plausible explanation for the observed inhibitory effects of AO-Ag NPs on bacterial strains at low doses.

On the other hand, the observed inhibitory effects may also be ascribed to the existence of negatively charged carboxyl and amino groups inside the peptidoglycan layer of the bacteria's cellular walls. The unique attribute that distinguishes AO-Ag NPs from traditional antibiotics is their remarkable efficacy in inhibiting bacterial growth.

Cytotoxic Assay Results

The cytotoxic effect of the produced biogenic silver nanoparticles (AO-Ag NPs) against five human cell lines, including four malignant cell lines and one healthy cell line, was evaluated using the MTT assay. Findings indicate that biogenic AO-Ag nanoparticles have remarkable cytotoxic effects on MDA-MB231, LnCap and A549 cancer cell lines, especially at a concentration of 50 mg/mL, as shown by EC_{50} values ranging from 15.15 ± 0.03 to 24.18 ± 0.07 $\mu g.mL^{-1}$ showed (Figure 7A–E). The human lung adenocarcinoma cell line (A549) had the highest sensitivity among the malignant cell lines, as indicated by an EC_{50} value of 15.15 ± 0.03 $\mu g.mL^{-1}$. Metallic nanoparticles have the potential to inhibit cell proliferation and induce apoptosis in rapidly proliferating cancer cells such as A549. Metallic nanoparticles generate

Table 3 Inhibitory Effect of AgNPs Obtained From Anchusa Officinalis Leaves on Pathogenic Microorganisms

Tested Pathogenic Microorganisms	AO-Ag NPs	Silver Nitrate (1 mM)	Standard Antibiotics* mg/L
S. aureus ATCC 29213; Gram (+)	0.5	2.65	2
Bacillus subtilis; Gram (+)	1.0	1.32	1
E. coli ATCC 25922; Gram (−)	0.5	0.66	2
Pseudomonas aeruginosa; Gram (−)	1.0	1.32	4
C. albicans	0.5	0.66	2

Notes: *Gram (+): Vancomycin (128 mg/mL); Gram (−) Colistin (128 μg/mL); Yeast: Fluconazole (128 μg/mL).

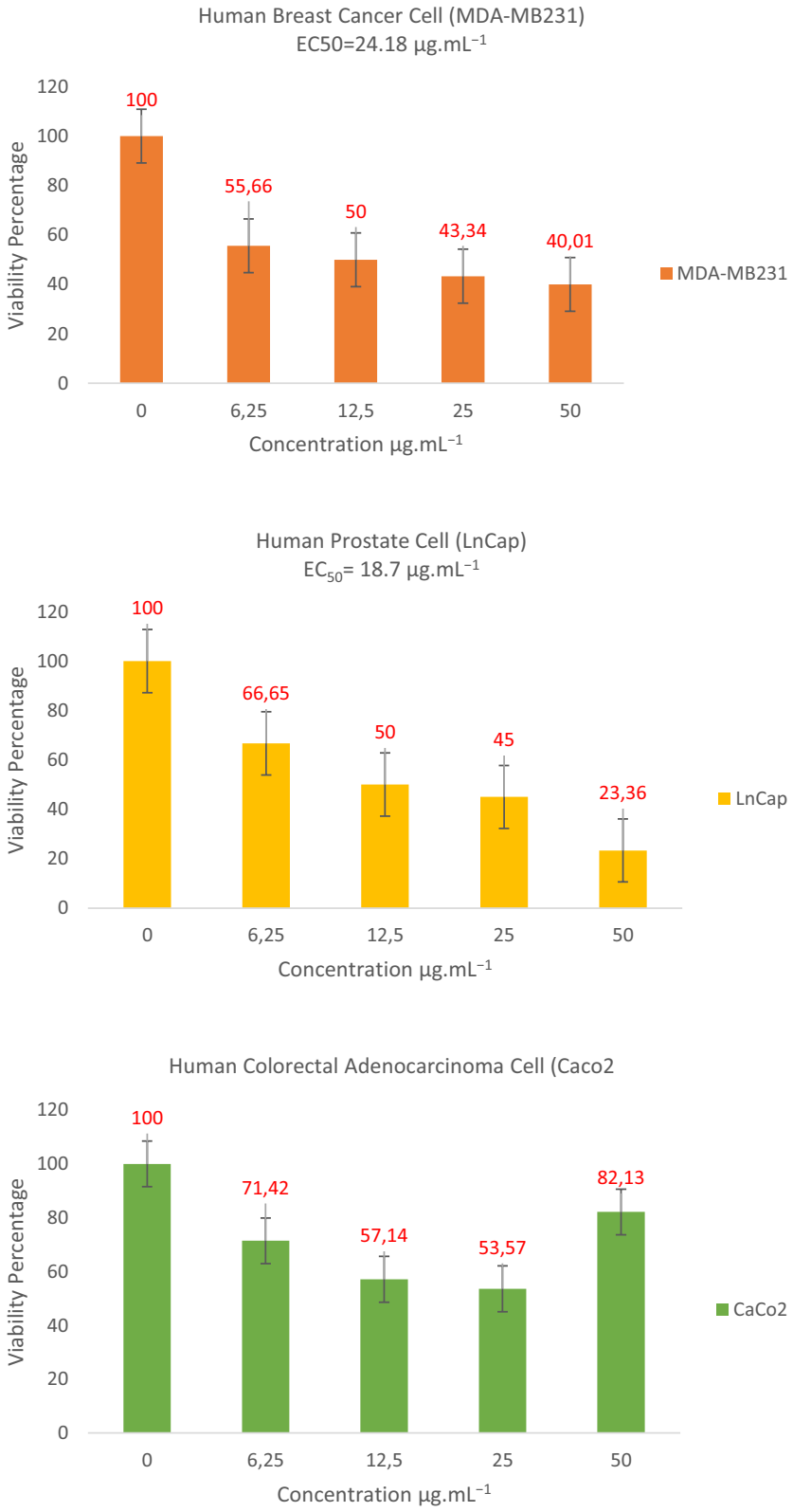

Figure 11 Continued.

https://doi.org/10.2147/IJN.S511217

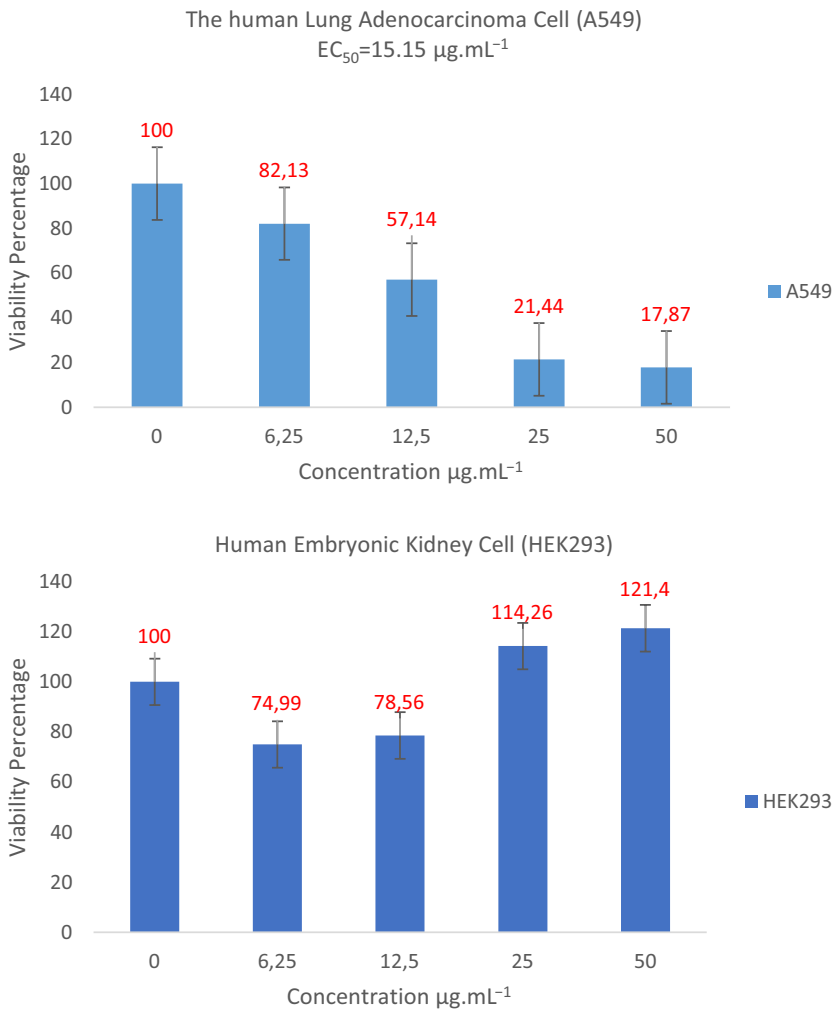

Figure 11 Viability rates of MDA-MB231, LnCap, A549, Caco-2, and HEK293 cell lines 24 hours after interaction with AO-Ag NPs.

ROS and have the potential to harm lipids, proteins, and DNA. A549 and other cancer cells are more vulnerable to ROS damage because of their altered redox balance and decreased capacity to withstand oxidative stress. The surface changes of metallic nanoparticles may enable them to target cancer cells by taking advantage of overexpressed receptors or markers such as A549.[72,73] Moreover, while the viability of human colorectal adenocarcinoma (Caco2) cells decreased significantly (71.42 ± 0.11 to 53.57 ± 0.09) in the concentration range of 6.25–25 µg/mL, the percentage of viability increased (83.12±0.15%) at 50 µg/mL concentration, showing proliferation. However, it was determined that the cytotoxic effect of AO-AgNPs on healthy human embryonic kidney (HEK293) cells was quite low at concentrations of 6.25 and 12.5 $\mu g.mL^{-1}$, on the contrary, it caused proliferation at concentrations of 25 and 50 µg/mL (Figure 11). Previous research revealed similar findings. According to Shaniba et al, AgNPs synthesized with *Manilkara zapota* exhibited potent anticancer effects on A549 cells.[74] Selvan et al reported that AgNPs synthesized with *Allium sativum* aqueous extract showed close anticancer activity against MCF7, A549, Hela and Hep2 cell lines.[75] The proliferation of the HEK 293 cell line was induced by an increase in the dose of silver nanoparticles. Nanoparticles may harm DNA, proteins, and lipids and generate elevated amounts of reactive oxygen species (ROS) inside cells. Apoptosis, necrosis, or cellular demise may ensue from this disruption of the cell cycle. Nevertheless, low quantities of reactive oxygen species may promote cell proliferation instead of inducing death. The activation of the MAPK (mitogen-activated protein kinase)/Erk1/2 (extracellular-regulated kinase 1/2) pathway in cancer, mediated by ROS, is facilitated by growth factors and K-ras and is functionally associated with enhanced cell proliferation.[76]

Conclusions

The environmental sustainability, biocompatibility, cost-effectiveness, and nanoparticle customization capabilities of plant-mediated synthesis make it significant. The vast diversification of plant species and their bioactive chemicals allows researchers to tailor nanoparticles for particular uses. Because they are safe and biocompatible, plant extract-derived nanoparticles are appealing for use in pharmaceutical and biomedical applications, opening the door to novel therapeutic and diagnostic strategies. However, in order to improve plant-mediated synthesis, more research is needed to address issues with uniformity, reproducibility, and scalability. For this sustainable method to be widely adopted throughout the industry, several issues must be resolved. Researchers are moving us closer to a time when ecological principles and nanotechnology coexist harmoniously to produce creative, ecologically friendly solutions by revealing the intricacies of plant-mediated synthesis. Silver nanoparticles (AgNPs) and their composites have unique physical and chemical characteristics that make them very promising for use in the medical field. The search for new plant extracts, microbial strains, or waste materials as reducing and stabilizing agents should continue to improve the environmental friendliness and cost-effectiveness of AgNP synthesis. At the same time, it is essential to optimize parameters such as pH, temperature, reaction time, and concentration of precursors to improve the yield, size control, and stability of nanomaterials. The role of capping agents in controlling particle size, shape, and stability and the use of microfluidic systems or templated synthesis to synthesize AgNPs with specific shapes and narrow size distributions should be developed. The generated biogenic AO-AgNPs' potent antibacterial action is most likely due to their capacity to overcome microbial resistance by combining physical, chemical, and biological mechanisms that target different cellular components and processes. The intricate relationship makes biogenic AgNPs more efficient antibacterial agents by preventing the development of resistance in microorganisms. Antibiotics are known to induce bacteria to develop various resistance mechanisms, and overuse of antibiotics is known to result in illness. In the medical field, using nanoparticles as an antibiotic substitute is becoming more and more common. However, it is well recognized that there are a variety of negative effects associated with nanoparticles that are not made by biological synthesis. The biological synthesis method is the suggested approach because it is not only economical and ecologically beneficial, but also healthful. The inhibition of cytotoxic action and the proliferation of malignant cell lines can be ascribed to a similar mechanism. *Anchusa officinalis* is unique among plant species that can be utilized in the biological production of nanoparticles due to its broad distribution, resilience to adverse environments, and abundant biochemical content. Similarly, it was found that the biosynthesis strategy, which uses the leaves of the Anchusa officinalis plant, was an appropriate way to generate Ag NPs. Furthermore, it successfully used the organic substances found in the plant's leaves as a silver salt reduction agent. The use of *A. officinalis* leaf extract as a capping reagent for the clean and green synthesis of silver metallic nanoparticles made this study novel. Significant antimicrobial and cytotoxic effects against pathogenic microorganisms and cancer cell lines were demonstrated by the obtained results, which advanced the field. Biogenic AO-Ag NPs are offered as an alternative to the conventional methods used in the treatment of infectious diseases and cancer because of their low cost and low toxicity. This implies that, with the right dosage modifications to treat particular illnesses, they may take the place of current antibiotic and anticancer medications. The efficacy of AO-AgNPs will be confirmed by further testing of the research using in vivo models or other cell lines and pathogen microorganisms.

Data Sharing Statement

All data used to support the findings of this study are included in the article. Samples of the compounds are available from the corresponding authors.

Acknowledgments

The authors are thankful to Mardin Artuklu University, Tabriz University of Medical Sciences, Batman University, and Ege University for providing all necessary research facilities to carry out this research.

Author Contributions

All authors made a significant contribution to the work reported, whether that is in the conception, study design, execution, acquisition of data, analysis and interpretation, or in all these areas; took part in drafting, revising or critically reviewing the article; gave final approval of the version to be published; have agreed on the journal to which the article has been submitted; and agree to be accountable for all aspects of the work.

Funding

C.K was supported by Mardin Artuklu University Scientific Research Unit (Grant no: MAÜ.BAP.21.SHMYO.099), and E. A was supported by the kidney research center of Tabriz University of Medical Sciences, Tabriz, Iran (Grant no: 73919).

Disclosure

The authors report no conflicts of interest in this work.

References

1. Kandav G, Sharma T. Green synthesis: an eco friendly approach for metallic nanoparticles synthesis. *Part Sci Technol*. 2024;42:874–894. doi:10.1080/02726351.2023.2281452
2. Salem SS, Fouda A. Green synthesis of metallic nanoparticles and their prospective biotechnological applications: an overview. *Biol Trace Elem Res*. 2021;199:344–370. doi:10.1007/s12011-020-02138-3
3. Mughal B, Zaidi SZJ, Zhang X, Hassan SU. Biogenic nanoparticles: synthesis, characterisation and applications. *Appl Sci*. 2021;11:2598.
4. Devi L, Kushwaha P, Ansari TM, Kumar A, Rao A. Recent trends in biologically synthesized metal nanoparticles and their biomedical applications: a review. *Biol Trace Elem Res*. 2023:1–17.
5. Vijayaram S, Razafindralambo H, Sun YZ, et al. Applications of green synthesized metal nanoparticles—a review. *Biol Trace Elem Res*. 2024;202:360–386. doi:10.1007/s12011-023-03645-9
6. Velidandi A, Dahariya S, Pabbathi NPP, Kalivarathan D, Baadhe RR. A review on synthesis, applications, toxicity, risk assessment and limitations of plant extracts synthesized silver nanoparticles. *NanoWorld J*. 2020;6(3):35–60. doi:10.17756/nwj.2020-079
7. Alharbi NS, Alsubhi NS, Felimban AI. Green synthesis of silver nanoparticles using medicinal plants: characterization and application. *J Radiat Res Appl Sci*. 2022;15:109–124.
8. Begum SJ, Pratibha S, Rawat JM, et al. Recent advances in green synthesis, characterization, and applications of bioactive metallic nanoparticles. *Pharma*. 2022;15:455.
9. Salem SS, Hammad EN, Mohamed AA, El-Dougdoug WA. Comprehensive review of nanomaterials: types, synthesis, characterization, and applications. *Biointerface Res Appl Chem*. 2022;13:41.
10. Khan F, Shariq M, Asif M, Siddiqui MA, Malan P, Ahmad F. Green nanotechnology: plant-mediated nanoparticle synthesis and application. *Nanomater*. 2022;12:673. doi:10.3390/nano12040673
11. Joudeh N, Linke D. Nanoparticle classification, physicochemical properties, characterization, and applications: a comprehensive review for biologists. *J Nanobiotechnology*. 2022;20:262. doi:10.1186/s12951-022-01477-8
12. Berhe MG, Gebreslassie YT. Biomedical applications of biosynthesized nickel oxide nanoparticles. *Int J Nanomed*. 2023;2023:4229–4251. doi:10.2147/IJN.S410668
13. Alqarni LS, Alghamdi MD, Alshahrani AA, Nassar AM. Green nanotechnology: recent research on bioresource-based nanoparticle synthesis and applications. *J Chem*. 2022;2022:1–31. doi:10.1155/2022/4030999
14. Naganthran A, Verasoundarapandian G, Khalid FE, et al. Synthesis, characterization and biomedical application of silver nanoparticles. *Materials*. 2022;15:427. doi:10.3390/ma15020427
15. Alowaiesh BF, Alhaithloul HAS, Saad AM, Hassanin AA. Green biogenic of silver nanoparticles using polyphenolic extract of olive leaf wastes with focus on their anticancer and antimicrobial activities. *Plants*. 2023;12:1410. doi:10.3390/plants12061410
16. Nicolae-Maranciuc A, Chicea D, Chicea LM. Ag nanoparticles for biomedical applications—synthesis and characterization—a review. *Int J Mol Sci*. 2022;23:5778. doi:10.3390/ijms23105778
17. Balkrishna A, Thakur N, Patial B, et al. Synthesis, characterization and antibacterial efficacy of *Catharanthus roseus* and Ocimum tenuiflorum-mediated silver nanoparticles: phytonanotechnology in disease management. *Processes*. 2023;11:1479. doi:10.3390/pr11051479
18. Xin X, Judy JD, Sumerlin BB, He Z. Nano-enabled agriculture: from nanoparticles to smart nanodelivery systems. *Environ Chem*. 2020;17:413–425. doi:10.1071/EN19254
19. Ali SS, Al-Tohamy R, Koutra E, et al. Nanobiotechnological advancements in agriculture and food industry: applications, nanotoxicity, and future perspectives. *Sci Total Environ*. 2021;792:148359. doi:10.1016/j.scitotenv.2021.148359
20. Salem SS. A mini review on green nanotechnology and its development in biological effects. *Arch Microbiol*. 2023;205:128. doi:10.1007/s00203-023-03467-2
21. Ndaba B, Roopnarain A, Haripriya RAMA, Maaza M. Biosynthesized metallic nanoparticles as fertilizers: an emerging precision agriculture strategy. *J Integr Agric*. 2022;21:1225–1242. doi:10.1016/S2095-3119(21)63751-6
22. Sengani M, Bavithra V, Banerjee M, et al. Evaluation of the anti-diabetic effect of biogenic silver nanoparticles and intervention in PPARγ gene regulation. *Environ Res*. 2022;215:114408. doi:10.1016/j.envres.2022.114408
23. Simon S, Sibuyi NRS, Fadaka AO, et al. Biomedical applications of plant extract-synthesized silver nanoparticles. *Biomedicines*. 2022;10:2792.
24. Alzubaidi AK, Al-Kaabi WJ, Ali AA, et al. Green synthesis and characterization of silver nanoparticles using flaxseed extract and evaluation of their antibacterial and antioxidant activities. *Appl Sci*. 2023;13:2182. doi:10.3390/app13042182

25. Husain S, Nandi A, Simnani FZ, et al. Emerging trends in advanced translational applications of silver nanoparticles: a progressing Dawn of nanotechnology. *J Funct Biomater*. 2023;14:47.
26. Patil MP, Kim GD. Eco-friendly approach for nanoparticles synthesis and mechanism behind antibacterial activity of silver and anticancer activity of gold nanoparticles. *Appl Microbiol Biotechnol*. 2017;101:79–92. doi:10.1007/s00253-016-8012-8
27. Vadakkan K, Rumjit NP, Ngangbam AK, Vijayanand S, Nedumpillil NK. Novel advancements in the sustainable green synthesis approach of silver nanoparticles (AgNPs) for antibacterial therapeutic applications. *Coord Chem Rev*. 2024;499:215528.
28. Islam R, Sun L, Zhang L. Biomedical applications of Chinese herb-synthesized silver nanoparticles by phytonanotechnology. *Nanomater*. 2021;11:2757.
29. Thatyana M, Dube NP, Kemboi D, Manicum ALE, Mokgalaka-Fleischmann NS, Tembu JV. Advances in phytonanotechnology: a plant-mediated green synthesis of metal nanoparticles using Phyllanthus plant extracts and their antimicrobial and anticancer applications. *Nanomater*. 2023;13:2616.
30. Khan AU, Hussain T, Abdullah-Khan MA, Almostafa MM, Younis NS, Yahya G. Antibacterial and antibiofilm activity of *Ficus carica*-mediated calcium oxide (CaONPs) phyto-nanoparticles. *Molecules*. 2023;28:5553. doi:10.3390/molecules28145553
31. Ekin I. Mineral and heavy metal concentration of nutritionally and therapeutically valued wild plants: insights into health effects. *Istanbul J Pharm*. 2022;52:179–186.
32. Hussain FHS, Ahamad J, Osw PS. A Comprehensive review on pharmacognostical and pharmacological characters of *Anchusa azurea*. *Adv Med Dent Health Sci*. 2019;3:33–37. doi:10.5530/amdhs.2019.3.10
33. Paun G, Neagu E, Albu C, Savin S, Radu GL. In vitro evaluation of antidiabetic and anti-inflammatory activities of polyphenolic-rich extracts from Anchusa officinalis and *Melilotus officinalis*. *ACS Omega*. 2020;5:13014–13022.
34. Boskovic I, Đukić DA, Maskovic P, Mandić L, Perovic S. Phytochemical composition and antimicrobial, antioxidant and cytotoxic activities of *Anchusa officinalis* L. extracts. *Biologia*. 2018;73:1035–1041.
35. Baran MF, Keskin C, Baran A, et al. Green synthesis of silver nanoparticles from *Allium cepa* L. peel extract, their antioxidant, antipathogenic, and anticholinesterase activity. *Molecules*. 2023;28(5):2310. doi:10.3390/molecules28052310
36. Keskin C, Ölçekçi A, Baran A, et al. Green synthesis of silver nanoparticles mediated *Diospyros kaki* L. (Persimmon): determination of chemical composition and evaluation of their antimicrobials and anticancer activities. *Front Chem*. 2023;11:1187808. doi:10.3389/fchem.2023.1187808
37. Dhaka A, Mali SC, Sharma S, Trivedi R. A review on biological synthesis of Silver nanoparticles and their potential applications. *Res Chem*. 2023;6:101108.
38. Khan T, Ali M, Khan A, et al. Anticancer plants: a review of the active phytochemicals, applications in animal models, and regulatory aspects. *Biomolecules*. 2019;10(1):47. doi:10.3390/biom10010047
39. Silviani D, Wahyuni WT, Syafitri UD, et al. LC-HRMS and FTIR-based metabolomics analysis and xanthine oxidase inhibitory evaluation of *Sida rhombifolia* with different drying methods. *Biocatal Agric Biotechnol*. 2023;52:102833. doi:10.1016/j.bcab.2023.102833
40. Behl T, Rocchetti G, Chadha S, et al. Phytochemicals from plant foods as potential source of antiviral agents: an overview. *Pharma*. 2021;14:381.
41. Terletskaya NV, Korbozova NK, Kudrina NO, et al. The influence of abiotic stress factors on the morphophysiological and phytochemical aspects of the acclimation of the plant *Rhodiola semenowii* Boriss. *Plants*. 2021;10:1196. doi:10.3390/plants10061196
42. Patel K, Patel DK. The beneficial role of rutin, a naturally occurring flavonoid in health promotion and disease prevention: a systematic review and update. *Bioact Food Dietary Interventions Arthritis Relat Inflamm Dis*. 2019:457–479.
43. Gullon B, Lú-Chau TA, Moreira MT, Lema JM, Eibes G. Rutin: a review on extraction, identification and purification methods, biological activities and approaches to enhance its bioavailability. *Trends Food Sci Technol*. 2017;67:220–235. doi:10.1016/j.tifs.2017.07.008
44. Yang LC, Chang YC, Yeh KL, Huang FM, Su NY, Kuan YH. Protective effect of rutin on triethylene glycol dimethacrylate-induced toxicity through the inhibition of caspase activation and reactive oxygen species generation in macrophages. *Int J Mol Sci*. 2022;23:11773. doi:10.3390/ijms231911773
45. Shabir S, Yousuf S, Singh SK, Vamanu E, Singh MP. Ethnopharmacological effects of Urtica dioica, Matricaria chamomilla, and Murraya koenigii on rotenone-exposed *D. melanogaster*: an attenuation of cellular, biochemical, and organismal markers. *Antioxidants*. 2022;11:1623. doi:10.3390/antiox11081623
46. Elansary O, Szopa H, Klimek-Szczykutowicz A, et al. Mammillaria species-polyphenols studies and anti-cancer, anti-oxidant, and anti-bacterial activities. *Molecules*. 2019;25:131. doi:10.3390/molecules25010131
47. Teng YN, Wang CC, Liao WC, Lan YH, Hung CC. Caffeic acid attenuates multi-drug resistance in cancer cells by inhibiting efflux function of human P-glycoprotein. *Molecules*. 2020;25:247. doi:10.3390/molecules25020247
48. Alfarrayeh I, Pollák E, Czéh A, Vida A, Das S, Papp G. Antifungal and anti-biofilm effects of caffeic acid phenethyl ester on different *Candida* species. *Antibiotics*. 2021;10(11):1359. doi:10.3390/antibiotics10111359
49. Zarmakoupi C, Mpistiolis K, Pantazis G, et al. Caffeic acid and biopesticides interactions for the control of storage beetles. *Appl Biosci*. 2023;2:211–221. doi:10.3390/applbiosci2020015
50. Khan F, Bamunuarachchi NI, Tabassum N, Kim YM. Caffeic acid and its derivatives: antimicrobial drugs toward microbial pathogens. *J Agric Food Chem*. 2021;69(10):2979–3004. doi:10.1021/acs.jafc.0c07579
51. Oršolić N, Kunštić M, Kukolj M, Odeh D, Ančić D. Natural phenolic acid, product of the honey bee, for the control of oxidative stress, peritoneal angiogenesis, and tumor growth in mice. *Molecules*. 2020;25:5583. doi:10.3390/molecules25235583
52. Wang M, Wang Z, Zhang J, et al. A matrine-based supramolecular ionic salt that enhances the water solubility, transdermal delivery, and bioactivity of salicylic acid. *Chem Eng J*. 2023;468:143480. doi:10.1016/j.cej.2023.143480
53. Song X, Li R, Zhang Q, He S, Wang Y. Antibacterial effect and possible mechanism of salicylic acid microcapsules against *Escherichia coli* and *Staphylococcus aureus*. *Int J Environ Res Public Health*. 2022;19:12761. doi:10.3390/ijerph191912761
54. Yeasmin F, Choi HW. Natural salicylates and their roles in human health. *Int J Mol Sci*. 2020;21(23):9049. doi:10.3390/ijms21239049
55. Le NPK, Herz C, Gomes JVD, et al. Comparative anti-inflammatory effects of Salix cortex extracts and acetylsalicylic acid in SARS-CoV-2 peptide and LPS-activated human in vitro systems. *Int J Mol Sci*. 2021;22:6766. doi:10.3390/ijms22136766
56. Geiger N, König EM, Oberwinkler H, et al. Acetylsalicylic acid and salicylic acid inhibit SARS-CoV-2 replication in precision-cut lung slices. *Vaccines*. 2022;10:1619. doi:10.3390/vaccines10101619

57. Alsharif SM, Salem SS, Abdel-Rahman MA, et al. Multifunctional properties of spherical silver nanoparticles fabricated by different microbial taxa. *Heliyon*. 2020;6(5):e03943. doi:10.1016/j.heliyon.2020.e03943
58. Ravichandran V, Vasanthi S, Shalini S, Shah SSA, Tripathy M, Paliwal N. Green synthesis, characterization, antibacterial, antioxidant and photocatalytic activity of Parkia speciosa leaves extract mediated silver nanoparticles. *Results Phys*. 2019;15:102565. doi:10.1016/j.rinp.2019.102565
59. Murali Krishna I, Bhagavanth Reddy G, Veerabhadram G, Madhusudhan A. Eco-friendly green synthesis of silver nanoparticles using Salmalia malabarica: synthesis, characterization, antimicrobial, and catalytic activity studies. *Appl Nanosci*. 2016;6:681–689. doi:10.1007/s13204-015-0479-6
60. Burlec AF, Corciova A, Boev M, et al. Current overview of metal nanoparticles' synthesis, characterization, and biomedical applications, with a focus on silver and gold nanoparticles. *Pharm*. 2023;16:1410.
61. El Megdar S, Fayzi L, Elkheloui R, et al. FTIR. *Curr Microbiol*. 2024;81:151. doi:10.1007/s00284-024-03670-4
62. Ibrahim E, Ahmad AA, Abdo ES, et al. Suppression of root rot fungal diseases in common beans (Phaseolus vulgaris L.) through the application of biologically synthesized silver nanoparticles. *Nanomaterials*. 2024;14:710. doi:10.3390/nano14080710
63. Said A, Abu-Elghait M, Atta HM, Salem SS. Antibacterial activity of green synthesized silver nanoparticles using Lawsonia inermis against common pathogens from urinary tract infection. *Appl Biochem Biotechnol*. 2024;196:85–98. doi:10.1007/s12010-023-04482-1
64. Hatipoğlu A, Baran A, Keskin C, et al. Green synthesis of silver nanoparticles based on the *Raphanus sativus* leaf aqueous extract and their toxicological/microbiological activities. *Environ Sci Pollut Res*. 2023;2023:1–13.
65. Fatima F, Aldawsari MF, Ahmed MM, et al. Green synthesized silver nanoparticles using tridax procumbens for topical application: excision wound model and histopathological studies. *Pharm*. 2021;13:1754.
66. Salvioni L, Galbiati E, Collico V, et al. Negatively charged silver nanoparticles with potent antibacterial activity and reduced toxicity for pharmaceutical preparations. *Int J Nanomed*. 2017;2017:2517–2530. doi:10.2147/IJN.S127799
67. Chinni SV, Gopinath SC, Anbu P, et al. Characterization and antibacterial response of silver nanoparticles biosynthesized using an ethanolic extract of *Coccinia indica* leaves. *Crystals*. 2021;11:97. doi:10.3390/cryst11020097
68. Dubey S, Virmani T, Yadav SK, Sharma A, Kumar G, Alhalmi A. Breaking barriers in eco-friendly synthesis of plant-mediated metal/metal oxide/bimetallic nanoparticles: antibacterial, anticancer, mechanism elucidation, and versatile utilizations. *J Nanomater*. 2024;2024:9914079. doi:10.1155/2024/9914079
69. Devanesan S, AlSalhi MS. Green synthesis of silver nanoparticles using the flower extract of Abelmoschus esculentus for cytotoxicity and antimicrobial studies. *Int J Nanomed*. 2021;2021:3343–3356. doi:10.2147/IJN.S307676
70. Rastegar F, Fallahi-Samberan M. Gelation of acrylic acid with Ag+ and conversion to Ag nanoparticle as potential system for biomedical applications. *Mater Chem Phys*. 2024;316:129042. doi:10.1016/j.matchemphys.2024.129042
71. Hu R, Deng L, Hao X, Chen J, Zhou X, Sahai N. Direct, broad-spectrum antimicrobial activity of Ag+-Doped hydroxyapatite against fastidious anaerobic periodontal and aerobic dental bacteria. *Materials*. 2024;17:4688. doi:10.3390/ma17194688
72. Andleeb A, Andleeb A, Asghar S, et al. A systematic review of biosynthesized metallic nanoparticles as a promising anti-cancer-strategy. *Cancers*. 2021;13:2818. doi:10.3390/cancers13112818
73. Martin A, Sarkar A. Overview on biological implications of metal oxide nanoparticle exposure to human alveolar A549 cell line. *Nanotoxicology*. 2017;11:713–724. doi:10.1080/17435390.2017.1366574
74. Shaniba VS, Aziz AA, Jayasree PR, Kumar PR. Manilkara zapota (L.) P. royen leaf extract derived silver nanoparticles induce apoptosis in human colorectal carcinoma cells without affecting human lymphocytes or erythrocytes. *Biol Trace Elem Res*. 2019;192:160–174. doi:10.1007/s12011-019-1653-6
75. Selvan DA, Mahendiran D, Kumar RS, Rahiman AK. Garlic, green tea and turmeric extracts-mediated green synthesis of silver nanoparticles: phytochemical, antioxidant and in vitro cytotoxicity studies. *J Photochem Photobiol B*. 2018;180:243–252. doi:10.1016/j.jphotobiol.2018.02.014
76. Liou GY, Storz P. Reactive oxygen species in cancer. *Free Radic Res*. 2010;44:79–496. doi:10.3109/10715761003667554